

Electrochemically induced CO₂ capture enabled by aqueous quinone flow chemistry

Yan Jing,^{1,2,3} Kiana Amini,^{2,3} Dawei Xi,² Shijian Jin,² Abdulrahman M. Alfaraidi,² Emily F. Kerr,¹ Roy G. Gordon,^{1,2*} Michael J. Aziz^{2*}

1. Department of Chemistry and Chemical Biology, Harvard University, Cambridge, Massachusetts 02138, United States
2. John A. Paulson School of Engineering and Applied Sciences, Harvard University, Cambridge, Massachusetts 02138, United States
3. These authors contributed equally to this work.

* E-mail: gordon@chemistry.harvard.edu; maziz@harvard.edu.

Abstract

Electrochemically-driven CO₂ capture processes utilizing redox-active organics in aqueous flow chemistry show promise for nonflammability, continuous-flow engineering, and the possibility of being driven at high current density by inexpensive, clean electricity. We show that the deprotonated hydroquinone–CO₂ adducts, whose insolubility limits the utility of the quinone–hydroquinone redox couple, become soluble when alkylammonium cations are introduced. Consequently, we introduce alkylammonium groups to anthraquinone via covalent bonds, making the resulting bis[3-(trimethylammonio)propyl]-anthraquinones (BTMAPAQs) soluble. We report the first aqueous quinone flow chemistry-enabled electrochemical CO₂ capture/release process, which occurs at ambient temperature and pressure, and show that it proceeds via both a pH-swing and a nucleophilicity-swing mechanism. 1,5-BTMAPAQ reaches the theoretical capture capacity of two CO₂ molecules per quinone from 1-bar CO₂–N₂ mixtures for which the CO₂ partial pressure is as low as 0.05 bar, or the applied current density is as high as 100 mA/cm², or the organic concentration is as high as 0.4 M. The energetic cost ranges from 48 to 140 kJ/molCO₂. In a crude simulated flue gas composed of 3% O₂, 10% CO₂, and 87% N₂, 1,5-BTMAPAQ electrolyte reversibly captured and released 50% of the theoretical capacity during an exposure of over 4 hr. It outperforms its isomeric counterparts 1,4-, and 1,8-BTMAPAQ in capture capacity and O₂ tolerance, demonstrating a substituent position effect on the reactivity of isomers with CO₂ and O₂. The results provide fundamental insight into electrochemical CO₂ capture with aqueous quinone flow chemistry and suggest that oxygen tolerance of reduced quinones may be significantly advanced through molecular engineering.

Accumulating atmospheric CO₂ concentrations from anthropogenic emissions compose the major source of global climate change. While progress is being made in switching from fossil fuel combustion to virtually emissions-free electricity sources, hard-to-abate sectors such as aviation and shipping will remain large sources of emissions for decades even in the most optimistic scenarios. Consequently, CO₂ removal – whether by capture from combustion exhaust or directly from the air or the ocean – is the subject of greatly increased attention, as it has become urgent to develop techniques that can be scaled up in a timely manner and globally deployed in the real world at reasonably low material and energetic cost.¹ Even after the attainment of a net zero emissions economy, it is likely that CO₂ removal will be desired in order to cut atmospheric concentrations toward pre-industrial levels. In an increasingly-electrified society, electrochemically-driven CO₂ capture at ambient conditions becomes an increasingly attractive option.^{2–5}

Quinones are ubiquitous electron-transfer carriers found in a range of living organisms.^{6,7} Featuring structural diversity, richness, and tunability as well as the earth-abundance of the compositional elements (C, H, O, N, S), quinones have been used as industrial dyes and for large-scale industrial production of hydrogen peroxide.^{8,9} Aqueous quinone flow batteries are approaching commercialization as a new generation of large-scale energy storage technique.¹⁰ Apart from energy storage, it has been reported that quinone cores can also be utilized for electrochemically induced carbon capture via two different mechanisms, depending on the use of solvents (Figure 1a). First, CO₂ can be directly chemisorbed by reduced quinones (Q²⁻), forming adducts [Q(CO₂)₂²⁻] in aprotic solvents.^{11,12} Second, quinones can undergo proton-coupled electron transfer (PCET) to be reduced to the hydroquinone form (H₂Q) in protic solvents,^{13–15} accompanied by the accumulation of hydroxide ions, indirectly leading to chemisorption of CO₂.^{16,17} For both mechanisms, the captured CO₂ can be reversibly released upon electrochemical oxidation. For simplicity, we name the first (direct) capture mechanism the nucleophilicity-swing mechanism and the second (indirect) capture mechanism the pH-swing mechanism. In both cases, a CO₂ capture–release cycle involves quinone reduction (an electron transfer process, abbreviated as *E*: Q + 2e⁻ → Q²⁻; Q + 2e⁻ + H₂O → HQ⁻ + OH⁻; Q + 2e⁻ + 2H₂O → H₂Q + 2OH⁻), CO₂ absorption (a chemical reaction, abbreviated as *C*: Q²⁻ + CO₂ → Q(CO₂)₂²⁻; HQ⁻ + CO₂ → HQ(CO₂)⁻; OH⁻ + CO₂ → HCO₃⁻), and concerted electrochemical oxidation and CO₂ release (*E*: Q(CO₂)₂²⁻ → Q

$+ 2\text{CO}_2 + 2\text{e}^-$; $\text{HQ}(\text{CO}_2)^- + \text{HCO}_3^- \rightarrow \text{Q} + \text{H}_2\text{O} + 2\text{CO}_2 + 2\text{e}^-$; $\text{H}_2\text{Q} + 2\text{HCO}_3^- \rightarrow \text{Q} + 2\text{CO}_2 + 2\text{H}_2\text{O} + 2\text{e}^-$). Therefore, both mechanisms undergo ECE processes in principle.

Quinones explored for CO_2 capture have been, almost without exception, immobilized on electrodes¹⁸⁻²¹ or dissolved in organic electrolytes.^{18,22,23} Solution-based capture inherits many of the advantages of flow batteries, including simple maintenance/top-off of active species, decoupled electrolyte activation and CO_2 capture, and continuous-flow engineering.²³⁻²⁷ In particular, aqueous electrolytes possess the advantage^{16,17,28-31} that water is non-flammable with virtually no cost; furthermore, high ionic conductivity of aqueous electrolytes allows high current density, enabling high areal throughput at ambient temperature and pressure. Combined, these advantages illustrate the opportunity for a capture system based on electrochemically-driven aqueous-soluble quinone flow chemistry. The sole aqueous-soluble quinone studied to date for CO_2 capture, disodium 4,5-dihydroxy-1,3-benzenedisulfonate (tiron), was studied only in static H-cells.^{15,32} One CO_2 per quinone was released via pH-swing caused by the electrochemical oxidation of tiron. Unfortunately, more than 60% of the initial capacity was lost after the first cycle due to the instability of the oxidized tiron molecule, which undergoes Michael addition and subsequent polymerization. To our knowledge, aqueous quinone flow chemistry-enabled electrochemical CO_2 capture and release has not previously been demonstrated.

Theoretically, to utilize a quinone for PCET-mediated electrochemical CO_2 capture cycle in aqueous electrolyte, the initial pH of the quinone electrolytes should be somewhat below $pK_{\text{a}1}$ of H_2CO_3 (~6), so that bicarbonate and carbonate concentrations are negligible compared to that of $\text{CO}_2(\text{aq})$. Upon electrochemical reduction, the quinone undergoes a PCET process, increasing the electrolyte pH until it reaches $pK_{\text{a}2}$ of the corresponding H_2Q ; upon further reduction of the electrolyte, the quinone undergoes zero-proton, two-electron transfer, generating Q^{2-} dianions without further altering the electrolyte pH.^{13,33} Because H_2Qs are weak acids and their pK_{a} values are usually less than 13,^{13,33,34} concentrated quinone electrolytes, when reduced, are expected to be predominantly in dianionic form rather than H_2Q form, favoring nucleophilicity-swing carbon capture. The two OH^- ions generated from the formation of hydroquinones would capture 1 or 2 CO_2 molecules via carbonate ($2\text{OH}^- + \text{CO}_2 \rightarrow \text{H}_2\text{O} + \text{CO}_3^{2-}$) or bicarbonate ($\text{OH}^- + \text{CO}_2 \rightarrow \text{HCO}_3^-$) formation. The two oxygen sites on the dianionic form of the reduced quinone can each bind one CO_2 molecule, yielding QCO_2^{2-} or $\text{Q}(\text{CO}_2)_2^{2-}$. Therefore, the CO_2 capture capacity of aqueous quinones is expected to range up to 2 CO_2 per quinone.

In general, aqueous quinones should meet several major criteria if used for electrochemical CO_2 capture. First, quinones should have high aqueous solubility in all states within their operational pH range. Second, the CO_2 -reactive reduced species, including H_2Q , HQ^- , Q^{2-} , and $\text{HQ}(\text{CO}_2)^-$, $\text{Q}(\text{CO}_2)_2^{2-}$, should resist reaction with O_2 long enough for most of the CO_2 capture capacity to be realized. Additionally, for the adduct formation mechanism, rate constants should be reasonably high and the binding constants should be high enough for most of the maximum capture capacity of 2 CO_2 per quinone to be attained, but not so high as to lead to unnecessarily large adduct oxidation potentials.

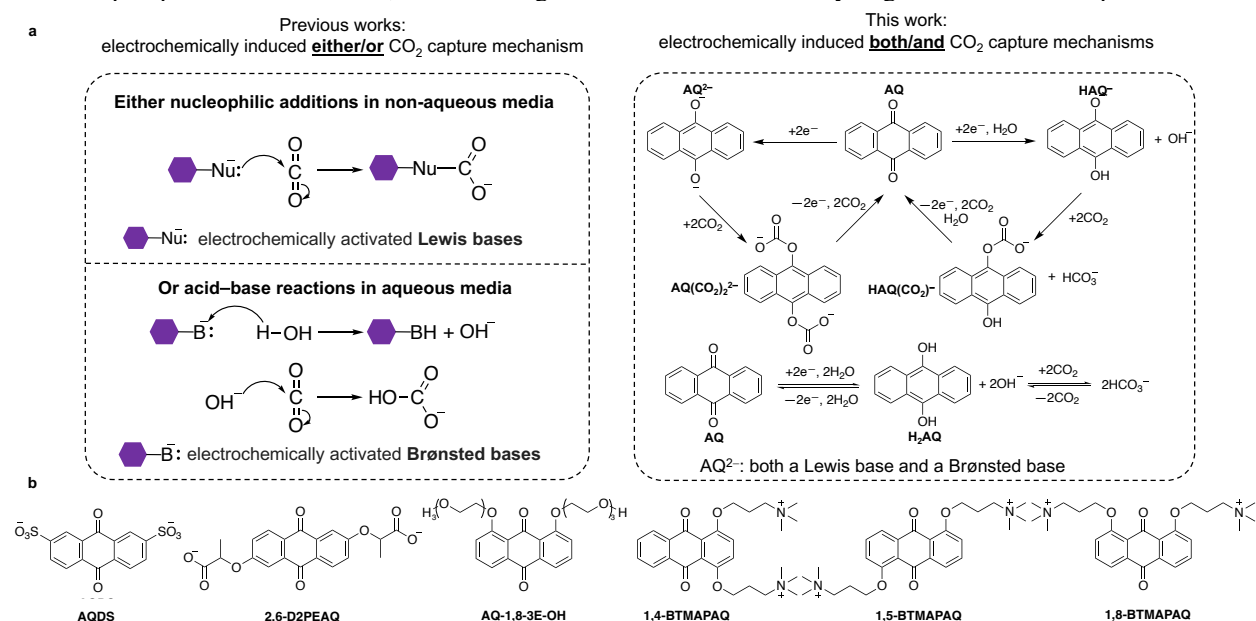


Figure 1 | (a) In previous works, electrochemical CO_2 capture in non-aqueous media is driven by electrochemically activated Lewis bases (nucleophiles) which undergo nucleophilic additions with CO_2 ;^{18,20,21,27} electrochemical CO_2

capture in aqueous media is driven by electrochemically activated Brønsted bases which undergo proton-coupled electron transfer induced acid–base reactions^{16,17,24,25,28,29,35,36}. In this work, electrochemical CO₂ capture with aqueous anthraquinone solutions is driven by AQ²⁻ which is both a Lewis base and a Brønsted base. The electrochemical CO₂ capture & release cycle involves both nucleophilicity- and pH-swing. (b) Six anthraquinone candidates that are soluble at neutral pH. Screened molecules: AQDS, 2,6-D2PEAQ, and AQ-1,8-3E-OH. Re-designed molecules: 1,4-, 1,5-, and 1,8-BTMAPAQ.

Informed by a decade of endeavors in developing aqueous anthraquinone flow batteries,³⁷⁻³⁹ we selected three anthraquinone derivatives that are aqueous-soluble at neutral pH: 2,7-disulfonated anthraquinone (AQDS),⁴⁰ 1,8-bis(2-(2-(2-hydroxyethoxy)ethoxy)ethoxy)anthracene-9,10-dione (AQ-1,8-3E-OH),³³ and 2,2'-((9,10-dioxo-9,10-dihydroanthracene-2,6-diyl)bis(oxy))-dipropionic acid (2,6-D2PEAQ)⁴¹ (Figure 1b). Although those quinones show > 1.0 M aqueous solubility in both oxidized and reduced states when used in flow batteries, bright yellow precipitates formed when CO₂ was introduced to the reduced electrolytes. The yellow precipitates did not form, and clear solutions were afforded when tetra-alkyl ammonium chlorides were used as the supporting salts (Figure 2, Table S1). Specifically, substituting 1 M NaCl with 1 M tetramethylammonium chloride (TMACl) as the supporting salt in 0.1 M AQDS electrolyte (Figure S1), replacing 1 M KCl with 1 M tetrabutylammonium chloride (TBACl) as the supporting salt in 0.1 M 2,6-D2PEAQ (Figure 2) or in 0.1 M AQ-1,8-3E-OH electrolytes produce transparent bright yellow solutions. One plausible explanation is that the bulky, amphiphilic tetra-alkyl ammonium cations and Q(CO₂)₂⁻ form loose ion pairs rather than the tight ion pairs between alkali metal cations and Q(CO₂)₂⁻.⁴² With the increased distance between Q(CO₂)₂⁻ and alkyl ammonium cations, the Coulomb attraction between the charges decreases, thereby raising the lattice energy and enhancing aqueous solubility.⁴³ However, the bulkiness of tetra-alkyl ammonium cations causes extremely high cell resistance (Figure S2a) in the flow cell systems because, in such cells, cation-exchange membranes must be used, resulting in prohibitively high energetic cost.

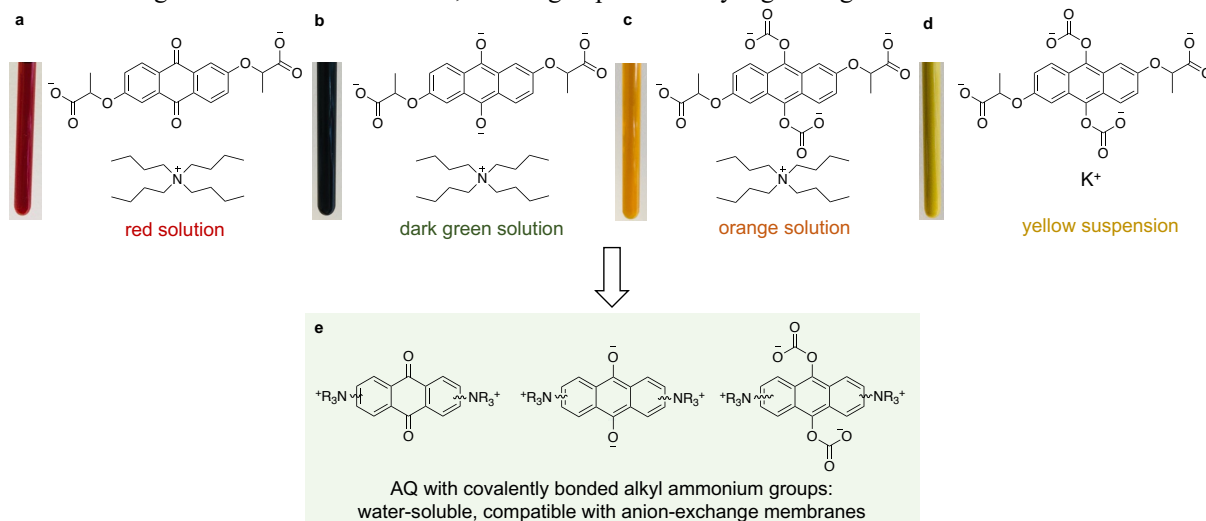


Figure 2 | Effect of supporting salt cations on solubility of $\text{Q}(\text{CO}_2)_2^{2-}$. (a) 0.1 M 2,6-D2PEAQ in 1 M TBACl; (b) 0.1 M reduced 2,6-D2PEAQ in 1 M TBACl; (c) 0.1 M reduced 2,6-D2PEAQ with saturated CO_2 in 1 M TBACl. (d) 0.1 M reduced 2,6-D2PEAQ with saturated CO_2 in 1 M KCl. (e) AQ possessing alkyl ammonium ending groups connected via covalent bonds, enhancing aqueous solubility and affording compatibility with anion-exchange membranes.

Inspired by the observation of dramatic change in aqueous solubility of reduced AQs in the presence of CO₂ caused by tetra-alkyl ammonium salts (Figure 2, Table S1), we hypothesized that anthraquinone derivatives tethered with bulky alkyl ammonium cations via covalent bonds might not only have high aqueous solubility in all states, but also be compatible with anion exchange membranes: the oxidized forms are positively charged and the reduced forms are charge-neutral but large in size, with correspondingly low expected cross-over rates. We designed and synthesized 1,4-, 1,5-, 1,8-,⁴⁴ and 2,6-bis[3-(trimethylammonio)propyl]-anthraquinone (BTMAPAQs) in which the numbers represent the positions of water-solubilizing chains (TMAP) bonded to anthraquinone (AQ) core. Of the four isomers, 2,6-BTMAPAQ exhibits very limited solubility (< 0.1 M) even in its oxidized state (Table S1); 1,8-BTMAPAQ(CO₂)₂²⁻ becomes soluble when TBA⁺ is used as the supporting salt cation (Figure S3); 1,4-, and 1,5-BTMAPAQs are soluble in all states even if KCl is used as the supporting salt. Therefore, 1,4-, 1,5-, and 1,8-BTMAPAQs (Figure 1b) were investigated for electrochemical CO₂ capture.

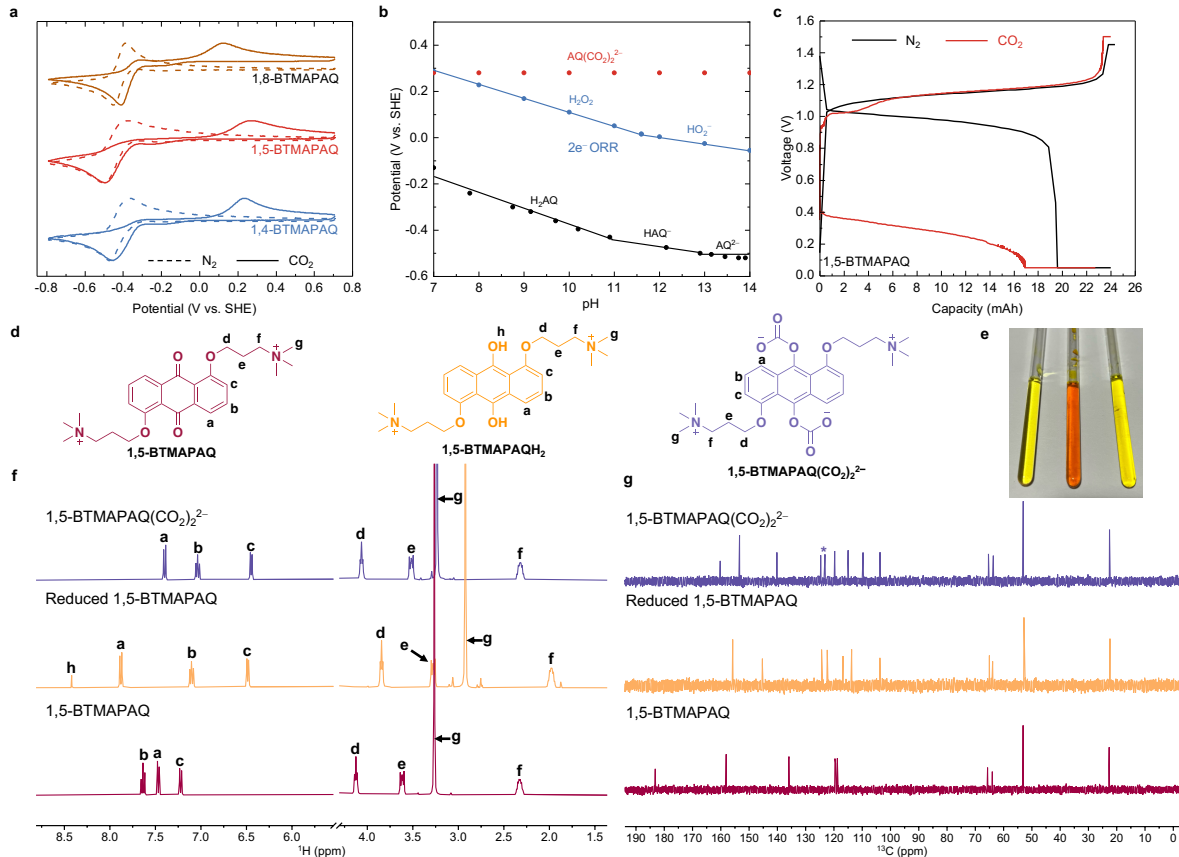


Figure 3 | Electrochemical and physiochemical characterization of BTMAPAQ in N_2 and CO_2 . (a) Cyclic voltammogram (CV) of 10 mL, 5 mM 1,4-, 1,5-BTMAPAQs in 1 M KCl, 5 mM 1,8-BTMAPAQ in 1 M KCl under streams of pure N_2 (dashed) or CO_2 (solid) at a scan rate of 100 mV s⁻¹. (b) Pourbaix diagram of 1,5-BTMAPAQ ($\text{AQ} + 2\text{e}^- + 2\text{H}_2\text{O} \rightarrow \text{H}_2\text{AQ} + 2\text{OH}^-$; $\text{AQ} + 2\text{e}^- + \text{H}_2\text{O} \rightarrow \text{HAQ}^- + \text{OH}^-$; $\text{AQ} + 2\text{e}^- \rightarrow \text{AQ}^{2-}$) and 2-electron oxygen reduction reaction ($\frac{1}{2}\text{O}_2 + 2\text{e}^- + \text{H}_2\text{O} \rightarrow \text{H}_2\text{O}_2$; $\frac{1}{2}\text{O}_2 + 2\text{e}^- + \text{H}_2\text{O} \rightarrow \text{HO}_2^- + \text{H}^+$). (c) Voltage profiles of 1,5-BTMAPAQ | FcNCl in 100% N_2 (black) and 10% CO_2 + 90% N_2 (red). During the charge–discharge process, a constant current density of 20 mA/cm² was first applied until the voltages approached the pre-set cutoffs. Potential holds were applied at 1.45 V for the charge in pure N_2 , 1.5 V for the charge in 90% N_2 and 10% CO_2 , and 0.05 V for the discharge until the current density decreased to 1 mA/cm². (d) Structure of 1,5-BTMAPAQ, 1,5-BTMAPAQH₂, and 1,5-BTMAPAQ(CO_2)₂²⁻. (e) NMR specimens, from left to right in the same order as the molecular structures in (d), and their ¹H NMR (f) and ¹³C NMR (g) spectra. Note that ¹H NMR peak broadening was initially observed from the electrochemically reduced aqueous quinone due to the occurrence of residual radicals, but addition of a tiny amount of HCl afforded well-defined peak splitting in the aromatic region (Figure 3f, orange). The chemical shift at 124.6 ppm in 1,5-BTMAPAQ(CO_2)₂²⁻ (Figure 3g, purple, identified with asterisk) is from the dissolved CO_2 .⁴⁵

Cyclic voltammetry (CV) was employed to investigate BTMAPAQs in buffered and unbuffered solutions. As shown in Figure 3a, at pH 7 in N_2 , 1,5-BTMAPAQ exhibits a redox potential of -0.465 V vs. SHE with a peak separation of 90 mV. When the solution was constantly purged with CO_2 , the major cathodic peak appears at -0.51 V along with a minor cathodic peak at -0.28 V (Figure 3a), which might be caused by a CO_2 buffering effect, enabling 1,5-BTMAPAQ to partially undergo a PCET process.¹³ The anodic peak of 1,5-BTMAPAQ largely shifts to $+0.28$ V, suggesting that extra energy is required to trigger the electrochemical oxidation: $1,5\text{-BTMAPAQ}(\text{CO}_2)_2^{2-} \rightarrow 1,5\text{-BTMAPAQ} + 2\text{CO}_2 + 2\text{e}^-$. Similar electrochemical behaviors were also shown by 1,4- and 1,8-BTMAPAQs.

To extract the relationship between redox potentials of 1,5-BTMAPAQ and electrolyte pH, we ran CVs in a series of buffered electrolytes to plot its Pourbaix diagram (Figure 3b). The $\text{pK}_{\text{a}1}$ and $\text{pK}_{\text{a}2}$ of 1,5-BTMAPH₂AQ are estimated at 10.9 and 12.8, consistent with other aqueous soluble anthrahydroquinones (H_2AQ).^{33,34,41} Because of the dominance of the nucleophilicity-swing mechanism in concentrated solutions, hereafter the oxidized, reduced, and CO_2 bonded states of quinones are abbreviated as Q, Q^{2-} , and $\text{Q}(\text{CO}_2)_2^{2-}$.

We assembled BTMAPAQs | (ferrocenylmethyl)trimethylammonium Chloride (FcNCl)⁴⁶ flow cells separated by anion-exchange membranes. Thanks to the compatibility between membrane and electrolytes, the alternating current area-specific resistance of the cells, measured via high-frequency electrochemical impedance spectroscopy, is as low as $\sim 1.5 \Omega \text{ cm}^2$ (Figure S4). While operating in 0.1 bar CO₂ and 0.9 bar N₂, we noticed a distinct discharge voltage decrease (Figure 3c, Figure S5), consistent with the anodic peak shifts in CVs (Figure 3a), confirming that Q(CO₂)₂²⁻ is the major product when the reduced form is exposed to CO₂. Interestingly, the color of BTMAPAQ solution changed dramatically in different states. For instance, 1,5-BTMAPAQ solution turned from bright yellow to light orange to pale yellow, corresponding to 1,5-BTMAPAQ, 1,5-BTMAPAQ²⁻, and 1,5-BTMAPAQ(CO₂)₂²⁻ (Figure 3e); the structure change was reflected by the distinct chemical shifts in both ¹H and ¹³C NMR spectra (Figure 3f, 3g). Dramatic color changes as well as distinct chemical shifts were also exhibited by AQDS and 1,8-BTMAPAQ in their corresponding three states (Figure S1, S3).

To examine the CO₂ capture capability of BTMAPAQs, we first conducted chemically induced CO₂ capture from pure, flowing CO₂, release into N₂, and sequestration as BaCO₃(s), from which we validated the CO₂ capture capacity of two CO₂ per quinone (Figure S6). Subsequently, we investigated the electrochemically induced CO₂ capture performance of 1,5-BTMAPAQ at 0.5 bar CO₂ and 0.5 bar N₂ (Figure 4a). The electrochemical reduction and oxidation were accompanied by CO₂ capture and release, which were reflected by the periodic oscillation of downstream CO₂ partial pressure and downstream gas flow rate, as well as the pH swing of 1,5-BTMAPAQ electrolyte. A 45-min. interval between reduction and oxidation was chosen as the minimum rest time to complete the gas-liquid reaction, which is the rate-limiting step (Figure S7). Integrating the downstream gas flow rate change during the CO₂ release indicates that the measured volume of released CO₂ is almost the same as the theoretical value (Figure S8), suggesting that each 1,5-BTMAPAQ can capture and release two CO₂ molecules. Through analyzing the round-trip voltage efficiency and coulombic efficiency over five cycles of the electrochemical reduction and oxidation, we found the energetic cost ranges from 65 to 80 kJ/molCO₂ at 20 mA/cm² at a fixed inlet CO₂ partial pressure of 0.5 bar. The close correspondence between the coulombic efficiency and the CO₂ release/capture efficiency in Figure S8e, defined as the ratio of the amount of CO₂ released to the amount captured in the immediately preceding half-cycle, indicates that CO₂ capture/release is triggered by the electrochemical reactions and mirrored by coulombic efficiencies.

In real applications, the partial pressure of CO₂ in feed gas varies over a broad range; hence we performed a series of tests in feed gas with varied partial pressure of CO₂ at 0.05, 0.1, 0.2, and 0.5 bars. To increase the CO₂ capture capacity, we adjusted the corresponding rest time intervals as 210, 105, 52, and 45 min., respectively (Figure 4a, Figure S9). During the electrochemical reduction of 1,5-BTMAPAQ, the pH range went from wide to narrow while the CO₂ partial pressure was adjusted from 0.05 to 0.5 bar. For instance, the pH swung from near neutral to ~ 12 at 0.05 bar CO₂, but to only ~ 9 at 0.5 bar CO₂. According to Henry's law, a higher partial pressure of CO₂ can lead to a higher CO₂ solubility in solution, thus enabling the prompt buffering of pH increase induced by electrochemical reduction. Despite of the variation in CO₂ partial pressure, two CO₂ molecules were captured by one 1,5-BTMAPAQ with energetic cost of 48 to 50 kJ/molCO₂ at 20 mA/cm².

One advantage of aqueous flow chemistry is the capability to operate electrochemical reactions at high current densities. Although extremely diluted CO₂ essentially limits the CO₂ capture heterogeneous chemical reaction rate regardless of technology, CO₂ release in our system is coupled with electrochemical oxidation; thus the CO₂ release rate can be readily accelerated by applying high current densities. We electrochemically reduced and oxidized 1,5-BTMAPAQ at 20, 40, 60, 80, and 100 mA/cm² in the presence of 0.1 bar CO₂ (Figure 4b, Figure S10). The depression of downstream CO₂ partial pressure and gas flow rate caused by CO₂ capture was almost the same at different current densities, indicating that CO₂ capture reaction rate is limited by mass transport of 0.1 bar CO₂ rather than by the electrochemical reduction rate, i.e., the applied current density. However, the peaks of downstream CO₂ partial pressure and gas flow rate caused by CO₂ release became sharper and narrower with the increase of current density, suggesting that the CO₂ release rate can be accelerated with increased current density, thus shortening the CO₂ release time. It is worth noting that the calculated volumes of the released CO₂ reach the theoretical values at different current densities (Figure S10). The mid-point voltage difference between charge and discharge curves increases with current density, which is caused by internal cell resistance, resulting in a broad energetic cost range of 65 to 140 kJ/molCO₂.

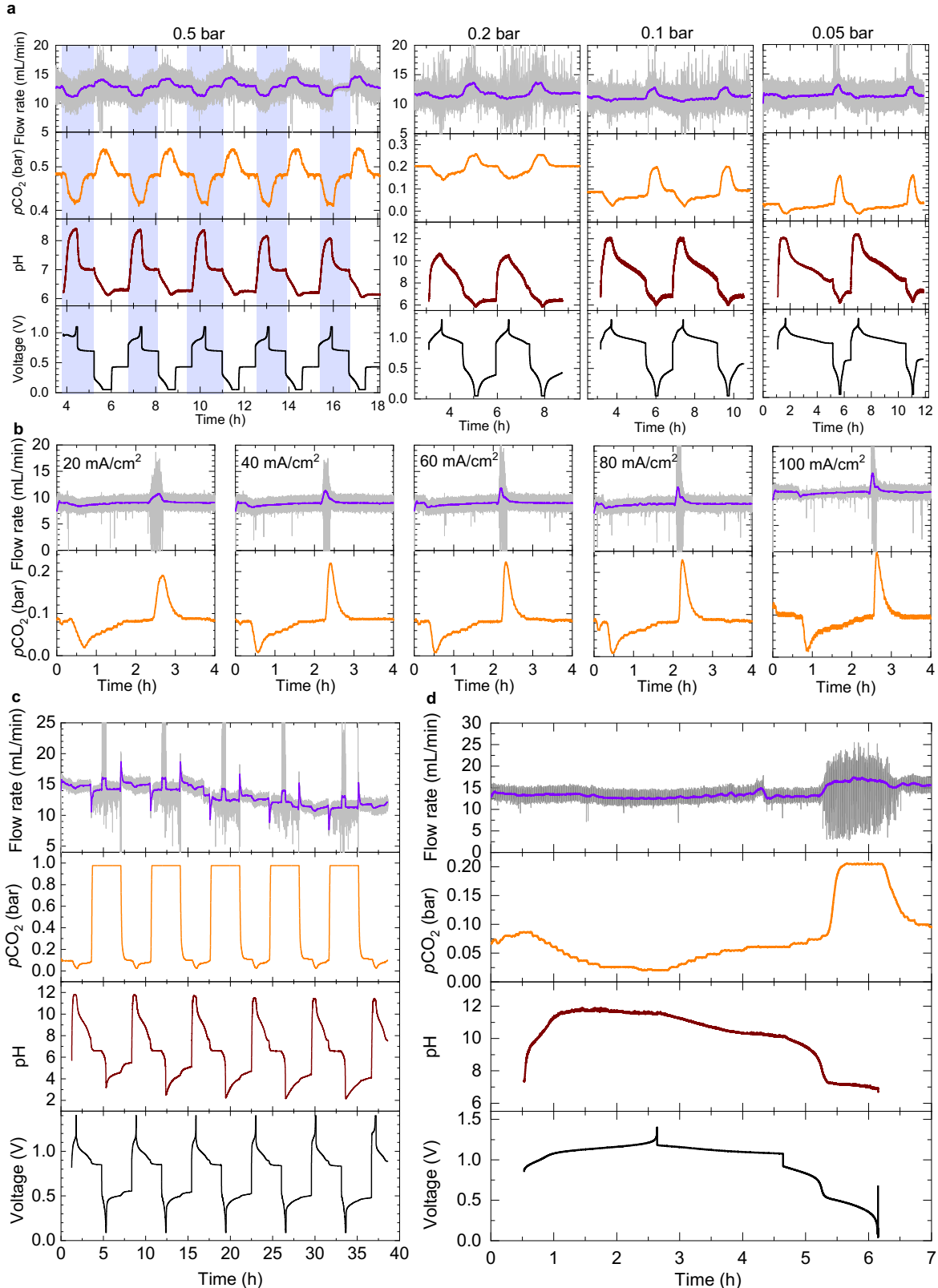


Figure 4 | 1,5-BTMAPAQ electrochemical CO_2 capture capability in $\text{CO}_2\text{-N}_2$ mixtures. (a) CO_2 capture and release cycling at $20 \text{ mA}/\text{cm}^2$. The partial pressure of CO_2 is set to $\approx 0.05, 0.1, 0.2$, and 0.5 bar for the experiments,

separately. The plots in Fig. 4a share the same Y-axis titles and units on the far left. Flow cells comprising 10–12 mL of 0.115 M 1,5-BTMAPAQ in 1 M KCl and 40 mL of 0.2 M FeNCl in 1 M KCl were used for the experiments at 0.05, 0.1 and 0.2 bar. A flow cell comprising 10 mL of 0.115 M 1,5-BTMAPAQ in 1 M KCl and 40 mL of 0.2 M BTMAPFc (bis((3-trimethylammonio)propyl)ferrocene dichloride)⁴⁷ in 1 M KCl was used for the experiment at 0.5 bar. (b) Plot presents the downstream CO₂ partial pressure and the downstream total gas flow rates when the electrochemical redox reactions were triggered at 20, 40, 60, 80, and 100 mA/cm². A flow cell comprises 10 mL of 0.057 M 1,5-BTMAPAQ in 1 M KCl and 40 mL of 0.1 M FeNCl in 1 M KCl. (c) CO₂ capture and release cycling where the capture occurred in an inlet CO₂ partial pressure of 0.1 bar and the release occurred in an inlet CO₂ partial pressure of 1 bar. A flow cell comprises 12 mL of 0.115 M 1,5-BTMAPAQ in 1 M KCl and 40 mL of 0.2 M FeNCl in 1 M KCl at 20 mA/cm². (d) CO₂ capture and release in inlet CO₂ partial pressure of 0.1 bar in a flow cell comprising 10 mL of 0.4 M 1,5-BTMAPAQ DI water and 30 mL of 0.9 M FeNCl in DI water at 20 mA/cm². Plots present current density, voltage, pH, downstream CO₂ partial pressure, and the downstream total gas flow rate of 1,5-BTMAPAQ electrolyte. The initial gas flow rate is set to 11.76 mL/min.

It is important to evaluate the CO₂ capture capacity and energetic cost when a system is used to capture CO₂ from a dilute source and release into pure CO₂. Hence, we performed our experiment using 1,5-BTMAPAQ with 0.1 bar inlet CO₂ and 1.0 bar pure CO₂ exit stream (Figure 4c). The volume of released CO₂ approaches the theoretical value over five cycles (Figure S12). The energetic cost and coulombic efficiency are either comparable to or slightly higher than those measured under previous conditions (Figure S9, S10, S11).

A concentrated quinone flow system comprising 0.4 M 1,5-BTMAPAQ was set up to demonstrate high volumetric CO₂ capture capacity (Figure 4d). Because of the low pKa values (<13) of 1,5-BTMAPH₂AQ (Figure 3b), the pH swing for 0.4 M 1,5-BTMAPAQ is the same as that for 0.1 M 1,5-BTMAPAQ, further supporting our interpretation of the results as the formation of Q(CO₂)₂²⁻. Although the increased concentration of 1,5-BTMAPAQ took a longer time to complete the capture, it still reaches the theoretical capacity at the energetic cost of 90 kJ/molCO₂.

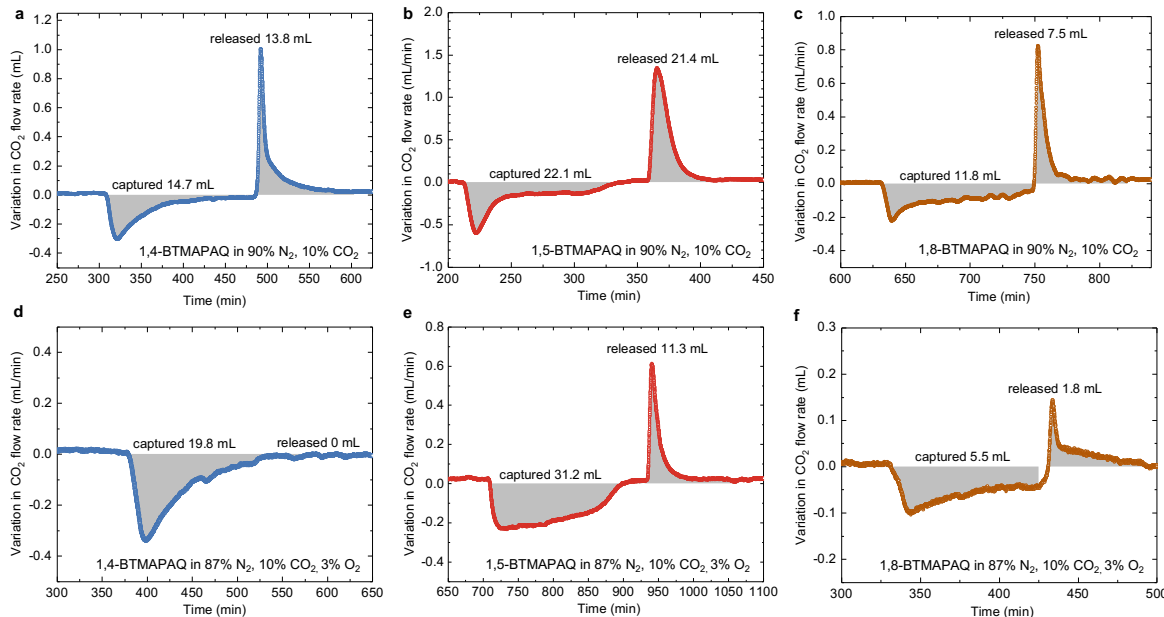


Figure 5 | CO₂ capture and release of 1,4-, 1,5-, 1,8-BTMAPAQs with and without O₂. Calculated volumes of captured and released CO₂ by (a) 1,4-, (b) 1,5-, (c) 1,8-BTMAPAQs in a feed gas stream of 90% N₂ and 10% CO₂ at 1.0 bar. Calculated volumes of captured and released CO₂ by (d) 1,4-, (e) 1,5-, (f) 1,8-BTMAPAQs in a feed gas stream of 87% N₂, 10% CO₂, and 3% O₂ (simulated flue gas) at 1.0 bar. 5 mL 0.1 M 1,4-, 1,5-BTMAPAQs, 1 M KCl solutions were paired with 40 mL 0.1 M FeNCl, 1 M KCl solution. 5 mL 0.1 M 1,8-BTMAPAQ 1 M TBACl solution was paired with 40 mL 0.1 M FeNCl, 1 M TBACl solution. The BTMAPAQs were electrochemically reduced and oxidized at 40 mA/cm² and followed by potential holds to complete the reactions. The theoretical CO₂ capture & release capacity for the BTMAPAQ electrolytes is 22.4 mL. Electrochemical reduction/oxidation were followed by rest time that was adjusted to approach the maximum CO₂ capture/release capacity while minimizing the O₂ induced side reactions. The durations of CO₂ capture/release for 1,4-BTMAPAQ are 175/125 min. without O₂ and 170/100 min. in the simulated gas, respectively. The durations of CO₂ capture/release for 1,5-BTMAPAQ are 145/80 min. without O₂

and 226/160 min. in the simulated gas, respectively. The durations of CO₂ capture/release for 1,8-BTMAPAQ are 120/90 min. without O₂ and 100/70 min. in the simulated gas, respectively. The addition of 1 M TBACl to 0.1 M 1,8-BTMAPAQ increased the viscosity of solution, slowing the dissolution of CO₂ and O₂ from gas phase to liquid phase.

In real applications, CO₂ always coexists with O₂ at varying partial pressures depending on CO₂ sources. It has been reported that reduced quinones are susceptible to O₂,^{23,48,49} which can reversibly chemically oxidize the reduced quinones to their oxidized states. These reduced quinones are the species of interest for binding CO₂. Hence, we investigated the oxygen sensitivity of the reduced quinones including H₂Q, HQ⁻, Q²⁻, HQ(CO₂)⁻, and Q(CO₂)²⁻, as capture will become practical only if the reduced quinones become oxidized by O₂ sufficiently slowly in an atmosphere with a relatively high O₂ partial pressure.

The reduced quinones are oxygen-sensitive because their oxidation potentials are much lower than the O₂ reduction potential. In contrast, the oxidation potentials of Q(CO₂)²⁻ can positively shift by at least 500 mV compared to those of the reduced quinones (Figure 3a), approaching the reduction potential of O₂ (Figure 3b) and possibly making Q(CO₂)²⁻ more O₂-tolerant. Through tracking ¹H NMR of the reduced quinones with and without captured CO₂ during air exposure (Figure S14–S19), we observed the reduced quinones gradually converted to the oxidized forms over days with different conversion rates. After operating BTMAPAQ flow cells in atmospheres with fixed CO₂ partial pressure but varied O₂ partial pressure (Table S2), we analyzed their coulombic efficiency to compare the oxygen sensitivity of BTMAPAQ isomers. We also performed chemically induced CO₂ capture, release, and sequestration with air exposure (Figure S20) and found that 1.7 equivalents of CO₂ were released when the solution with captured CO₂ was vigorously stirred in air for 15 min. The detailed information is reported in the Oxygen sensitivity section of Supplementary Information. Those measurements inspired us to further evaluate BTMAPAQs-based electrochemical CO₂ capture from simulated flue gases with an upgraded system setup (Figure S21–S23). By integrating the peak area of CO₂ flow rate deviation over CO₂ capture and release cycles (Figure 5), we evaluated the CO₂ capture and release volumes from 1,4-, 1,5-, and 1,8-BTMAPAQs in the absence and presence of O₂. When 1,4- and 1,5-BTMAPAQ were exposed to 1.0 bar feed gas composed of 10% CO₂ and 90% N₂, the CO₂ release/capture volume ratio is close to 1 (Figure 5a, 5b), suggesting the reversibility of CO₂ capture and release. When exposed to 1.0 bar simulated flue gas composed of 3% O₂, 10% CO₂, and 87% N₂, the volumes of released CO₂ greatly decrease, which we attribute to the oxygen-induced side reactions shown in Eqns. 10 and 11 in Table 1. Compared to the CO₂ capture volumes from 1,4- and 1,5-BTMAPAQs in the absence of O₂, their CO₂ capture volumes in the presence of O₂ become significantly larger, which we attribute to additional CO₂ irreversibly trapped by the hydroxide ions converted from oxygen (Eqns. 7, 8, 10, and 11 in Table 1). The superior oxygen tolerance shown by 1,5-BTMAPAQ might be due to its net zero dipole moment and the overall non-polar structure. Polar molecules tend to have higher reactivity,⁵⁰ which may explain the inferior oxygen tolerance shown by 1,4- and 1,8-BTMAPAQs. The CO₂ capture volumes from 1,8-BTMAPAQ are much smaller than those from 1,4- and 1,5-BTMAPAQ, which we tentatively attribute to the increased electrolyte viscosity caused by the addition of 1 M TBA⁺, which slows down the dissolution of CO₂ to the electrolyte, lowering the capture capacity.

Among the three BTMAPAQ isomers, 1,5-BTMAPAQ shows the highest CO₂ capture capacity of 21.4 mL in the absence of O₂, which is close to the theoretical value of 22.4 mL assuming one 1,5-BTMAPAQ captures two CO₂ molecules. Under 3% O₂ exposure for 226 min. during CO₂ capture and 160 min. during the release, 1,5-BTMAPAQ still released 11.3 mL CO₂, which is ~50% of the theoretical capacity. It is worth noting that the CO₂ capture/release capacity can be further improved by optimizing the CO₂ capture time duration, as with decreased exposure time there should be fewer O₂-induced side reactions, and more captured CO₂ will be released. However, if the CO₂ capture duration is too short, both captured and released CO₂ volumes will become small, lowering the faradaic efficiency, defined in this context as the ratio of the amount of CO₂ reversibly captured and released to the theoretical capacity. Thus, a trade-off is apparent between the CO₂ release/capture volume ratio and faradic efficiency. Nevertheless, the O₂ resistance and CO₂ capture capability shown by 1,5-BTMAPAQ in Figure 5e demonstrates that reduced quinones are not necessarily too oxygen-sensitive to be useful for CO₂ capture. The BTMAPAQ-based electrochemical CO₂ capture–release behavior in a simulated flue gas atmosphere over multiple cycles (Figure S24–S27) illustrates that there is still room for improvement of long-term O₂-tolerance of reduced quinones through judicious molecular design. The distinct O₂ reactivity difference among the isomers implies that a substituent position effect plays a major role in governing their oxygen tolerance. The substituent positions in the isomers may affect the interaction strength between the positively charged alkylammonium ending groups and the negatively charged phenolate active sites or the organic adducts, further influencing the nucleophilicity-induced CO₂ capture capacity and O₂-induced chemical redox reactions.

Table 1 | Electrochemical and chemical reactions during CO₂ capture & release when oxygen is involved. The hydroxide ions produced from Eqns. 7 and 8 can irreversibly capture CO₂ via Eqn 6. The captured CO₂ can escape due to the chemical oxidation shown in Eqns. 10 and 11.

Stage 1	Electrochemical reduction	Eqn. 1	AQ + 2e ⁻ → AQ ²⁻
		Eqn. 2	AQ + 2e ⁻ + 2H ₂ O → H ₂ AQ + 2OH ⁻
		Eqn. 3	AQ + 2e ⁻ + H ₂ O → HAQ ⁻ + OH ⁻
Stage 2	Electrochemically induced CO ₂ capture	Eqn. 4	AQ ²⁻ + CO ₂ → AQ(CO ₂) ²⁻
		Eqn. 5	HAQ ⁻ + CO ₂ → HAQ(CO ₂) ⁻
		Eqn. 6	OH ⁻ + CO ₂ → HCO ₃ ⁻
Stage 2	O ₂ -involved chemical reactions lead to irreversible capture and escape of CO ₂	Eqn. 7	AQ ²⁻ + H ₂ O + 1/2O ₂ → AQ + 2OH ⁻
		Eqn. 8	HAQ ⁻ + 1/2O ₂ → AQ + OH ⁻
		Eqn. 9	H ₂ AQ + 1/2O ₂ → AQ + H ₂ O
		Eqn. 10	HAQ(CO ₂) ⁻ + 1/2O ₂ → AQ + OH ⁻ + CO ₂
		Eqn. 11	AQ(CO ₂) ²⁻ + H ₂ O + 1/2O ₂ → AQ + 2OH ⁻ + 2CO ₂
Stage 3	Electrochemically induced CO ₂ release	Eqn. 12	AQ(CO ₂) ²⁻ - 2e ⁻ → AQ + 2CO ₂
		Eqn. 13	H ₂ AQ - 2e ⁻ + 2HCO ₃ ⁻ → AQ + 2H ₂ O + 2CO ₂
		Eqn. 14	HAQ(CO ₂) ⁻ - 2e ⁻ + HCO ₃ ⁻ → AQ + H ₂ O + 2CO ₂

More broadly, molecular oxygen tolerance can be improved via molecular engineering with the incorporation of steric and electronic effects, intra-molecular interactions, *etc.* induced by quinone cores or covalently bonded functional groups. The both basicity and nucleophilicity-based CO₂ capture mechanisms further enlarge the molecular design space, facilitating the discovery of desired molecules.

1. **Steric hindrance** could be introduced to prevent the chemical oxidation between activated molecules and molecular oxygen. Note that the introduction of steric hindrance will make the nucleophilic addition between activated molecules and CO₂ difficult without affecting the basicity of activated molecules, leading to the dominance of pH-swing based CO₂ capture & release.
2. **Intramolecular hydrogen bonding** can potentially stabilize activated molecules, making them difficult to be oxidized by O₂. Apaydin *et al.*⁵¹ has demonstrated that an activated quinacridone film with captured CO₂ via nucleophilic addition can be stabilized by hydrogen bonds, in which CO₂ can be released only with extra heat, or at an applied oxidation potential of 0.7 V vs. Fc/Fc⁺, which is substantially higher than the oxygen reduction potential (-1.2 V vs. Fc/Fc⁺).²⁷ It is thus possible that intramolecular hydrogen bonds can also stabilize activated molecules in solutions.
3. **Elevating the oxidation potentials of activated molecules** above the oxygen reduction potential should make them oxygen-tolerant. Meanwhile, increasing potentials might also decrease the basicity and nucleophilicity of activated molecules, thus making them less capable to capture CO₂ via either mechanism, compromising their CO₂ capture capacity.⁴⁸
4. **Lowering the oxidation potentials of activated molecules** may be a counterintuitive approach to increase oxygen-tolerance of activated molecules. When the Gibbs free energy of chemical redox reaction between activated molecules and O₂ is too negative and falling into the Marcus inverted region, the reaction rate will decrease as the driving force increases.⁵²
5. **Machine learning** is emerging as a powerful approach in materials discovery.⁵³ It thus has potential to offer valuable guidelines and accelerate the discovery of oxygen-tolerant redox molecules.

Through molecular screening and modification, we developed three water-soluble and anion-exchange membrane compatible bis[3-(trimethylammonio)propyl]-anthraquinone (BTMAPAQ) isomers that can be used for electrochemical CO₂ capture. With a series of characterizations including cyclic voltammetry, Pourbaix diagram analysis, ¹H and ¹³C NMR, electrochemical charge-discharge voltage-capacity profiles, and in situ monitoring of pH, pCO₂, and gas flow rate, we showed that aqueous quinone flow chemistry-enabled electrochemical CO₂ capture proceeds via pH-swing and nucleophilicity-swing mechanisms. The latter is more dominant because of low pKa values of hydroquinones. 1,5-BTMAPAQ electrolyte can capture and release the theoretical limit of two equivalents of CO₂ molecules per quinone from 1-bar CO₂-N₂ mixtures for which the CO₂ partial pressure is as low as 0.05 bar, or the applied current density is as high as 100 mA/cm², or the organic concentration is as high as 0.4 M, with an energetic cost ranging from 48 to 140 kJ/molCO₂. When exposed to a simulated flue gas comprising 3% O₂, 10% CO₂, and 87%

N_2 at 1.0 bar total pressure for over 4 hr., 1,5-BTMAPAQ reversibly captured and released 50% of the theoretical capacity. The distinct position effect on O_2 reactivity exhibited by BTMAPAQ isomers illustrates the opportunity for molecular engineering for further improvement of molecular properties. This may stimulate the progress of oxygen-tolerant, low-cost, scalable aqueous quinone flow chemistry enabled electrochemical CO_2 capture.

Present Addresses:

[#]Y. J.: National University of Singapore, 117575, Singapore

^{\$}K. A.: University of British Columbia, Vancouver, BC Canada V6T 1Z4

[†]Shijian Jin: X, the moonshot factory, Mountain View, California, United States

[§]Emily F. Kerr: Xavier University, Cincinnati, OH 45207, United States

Supporting Information

General experimental procedures; solubility of anthraquinones; oxygen sensitivity of reduced anthraquinones; chemical CO_2 capture, release, and sequestration in the absence/presence of O_2 ; electrochemical CO_2 capture in the absence/presence of O_2 .

Acknowledgments

Research at Harvard was supported by the Harvard Climate Change Solutions Fund. K.A. was supported in part by U.S. DOE award DE-AC05-76RL01830 through PNNL subcontract 654799 and in part through the Natural Sciences and Engineering Research Council of Canada (NSERC) Postdoctoral Fellowship (PDF) program [application number PDF-557232-2021]. We acknowledge Alexander Forse from Univ. of Cambridge for useful discussions. We thank Prof. Theodore A. Betley, Dr. Thomas Cochard, Andrew Bergman, Toly Rinberg, Eric M. Fell, Thomas Y. George, Maia Alberts, Michael Emanuel, Dr. Tatsuhiko Tsukamoto, Dr. Jinxu Gao for useful discussions.

Competing interests

The authors declare no competing interests.

Correspondence and requests for materials should be addressed to Michael J. Aziz.

References

- ¹K.Z. House, A.C. Baclig, M. Ranjan, E.A. van Nierop, J. Wilcox, and H.J. Herzog, "Economic and Energetic Analysis of Capturing CO_2 from Ambient Air", *Proc. Natl. Acad. Sci. USA* **108**, 20428 (2011). <https://doi.org/10.1073/pnas.1012253108>
- ²A.M. Zito, L.E. Clarke, J.M. Barlow, D. Bim, Z. Zhang, K.M. Ripley, C.J. Li, A. Kummeth, M.E. Leonard, A.N. Alexandrova, F.R. Brushett, and J.Y. Yang, "Electrochemical Carbon Dioxide Capture and Concentration", *Chem. Rev.* **123**, 8069 (2023). <https://doi.org/10.1021/acs.chemrev.2c00681>
- ³K.M. Diederichsen, R. Sharifian, J.S. Kang, Y. Liu, S. Kim, B.M. Gallant, D. Vermaas, and T.A. Hatton, "Electrochemical Methods for Carbon Dioxide Separations", *Nature Reviews Methods Primers* **2**, 68 (2022). <https://doi.org/10.1038/s43586-022-00148-0>
- ⁴M. Rahimi, A. Khurram, T.A. Hatton, and B. Gallant, "Electrochemical Carbon Capture Processes for Mitigation of CO_2 Emissions", *Chem. Soc. Rev.* **51**, 8676 (2022). <https://doi.org/10.1039/d2cs00443g>
- ⁵J.M. Barlow, L.E. Clarke, Z. Zhang, D. Bim, K.M. Ripley, A. Zito, F.R. Brushett, A.N. Alexandrova, and J.Y. Yang, "Molecular Design of Redox Carriers for Electrochemical CO_2 Capture and Concentration", *Chem. Soc. Rev.* **51**, 8415 (2022). <https://doi.org/10.1039/d2cs00367h>
- ⁶P.J. O'Brien, "Molecular Mechanisms of Quinone Cytotoxicity", *Chem.-Biol. Interactions* **80**, 41 (1991). [https://doi.org/https://doi.org/10.1016/0009-2797\(91\)90029-7](https://doi.org/https://doi.org/10.1016/0009-2797(91)90029-7)
- ⁷B. Nowicka and J. Kruk, "Occurrence, Biosynthesis and Function of Isoprenoid Quinones", *Biochim Biophys Acta* **1797**, 1587 (2010). <https://doi.org/10.1016/j.bbabi.2010.06.007>
- ⁸B. Dulo, K. Phan, J. Githaiga, K. Raes, and S. De Meester, "Natural Quinone Dyes: A Review on Structure, Extraction Techniques, Analysis and Application Potential", *Waste and Biomass Valorization* **12**, 6339 (2021). <https://doi.org/10.1007/s12649-021-01443-9>
- ⁹J.M. Campos-Martin, G. Blanco-Brieva, and J.L. Fierro, "Hydrogen Peroxide Synthesis: An Outlook Beyond the Anthraquinone Process", *Angew. Chem. Int. Ed. Engl.* **45**, 6962 (2006). <https://doi.org/10.1002/anie.200503779>
- ¹⁰Y. Jing, R.G. Gordon, and M.J. Aziz, "Aqueous Organic Flow Batteries.", *Weinheim: Wiley-VCH* **3**, (2023).

- ¹¹M.B. Mizen and M.S. Wrighton, "Reductive Addition of CO₂ to 9,10-Phenanthrenequinone", *Journal of the Electrochemical Society* **136**, 7 (1989). <https://doi.org/https://doi.org/10.1149/1.2096891>
- ¹²P. Scovazzo, J. Poshusta, D. DuBois, C. Koval, and R. Noble, "Electrochemical Separation and Concentration of 1% CO₂ from Nitrogen", *Journal of the Electrochemical Society* **150**, 8 (2003). <https://doi.org/https://doi.org/10.1149/1.1566962>
- ¹³M. Quan, D. Sanchez, M.F. Wasylkiw, and D.K. Smith, "Voltammetry of Quinones in Unbuffered Aqueous Solution: Reassessing the Roles of Proton Transfer and Hydrogen Bonding in the Aqueous Electrochemistry of Quinones", *J. Am. Chem. Soc.* **129**, 12847 (2007). <https://doi.org/10.1021/ja0743083>
- ¹⁴J.D. Watkins, N.S. Siebert, X. Zhou, C.R. Myers, J.R. Kitchin, D.P. Hopkinson, and H.B. Nulwala, "Redox-Mediated Separation of Carbon Dioxide from Flue Gas", *Energy & Fuels* **29**, 7508 (2015). <https://doi.org/10.1021/acs.energyfuels.5b01807>
- ¹⁵C.L. Huang, C.J. Liu, K.J. Wu, H.R. Yue, S.Y. Tang, H.F. Lu, and B. Liang, "CO₂ Capture from Flue Gas Using an Electrochemically Reversible Hydroquinone/Quinone Solution", *Energy & Fuels* **33**, 3380 (2019). <https://doi.org/10.1021/acs.energyfuels.8b04419>
- ¹⁶S. Jin, M. Wu, R.G. Gordon, M.J. Aziz, and D.G. Kwabi, "pH Swing Cycle for CO₂ Capture Electrochemically Driven through Proton-Coupled Electron Transfer", *Energy & Environmental Science* **13**, 3706 (2020). <https://doi.org/10.1039/d0ee01834a>
- ¹⁷H. Xie, W. Jiang, T. Liu, Y. Wu, Y. Wang, B. Chen, D. Niu, and B. Liang, "Low-Energy Electrochemical Carbon Dioxide Capture Based on a Biological Redox Proton Carrier", *Cell Reports Physical Science* **1**, 100046 (2020). <https://doi.org/10.1016/j.xrps.2020.100046>
- ¹⁸B. Gurkan, F. Simeon, and T.A. Hatton, "Quinone Reduction in Ionic Liquids for Electrochemical CO₂ Separation", *ACS Sustainable Chemistry & Engineering* **3**, 1394 (2015). <https://doi.org/10.1021/acssuschemeng.5b00116>
- ¹⁹D. Wielend, D.H. Apaydin, and N.S. Sariciftci, "Anthraquinone Thin-Film Electrodes for Reversible CO₂ Capture and Release", *Journal of Materials Chemistry A* **6**, 15095 (2018). <https://doi.org/10.1039/c8ta04817g>
- ²⁰S. Voskian and T.A. Hatton, "Faradaic Electro-Swing Reactive Adsorption for CO₂ Capture", *Energy & Environmental Science* **12**, 3530 (2019). <https://doi.org/10.1039/c9ee02412c>
- ²¹Y. Liu, H.Z. Ye, K.M. Diederichsen, T. Van Voorhis, and T.A. Hatton, "Electrochemically Mediated Carbon Dioxide Separation with Quinone Chemistry in Salt-Concentrated Aqueous Media", *Nat. Commun.* **11**, 2278 (2020). <https://doi.org/10.1038/s41467-020-16150-7>
- ²²K.M. Diederichsen, Y. Liu, N. Ozbek, H. Seo, and T.A. Hatton, "Toward Solvent-Free Continuous-Flow Electrochemically Mediated Carbon Capture with High-Concentration Liquid Quinone Chemistry", *Joule* **6**, 221 (2022). <https://doi.org/10.1016/j.joule.2021.12.001>
- ²³J.M. Barlow and J.Y. Yang, "Oxygen-Stable Electrochemical CO₂ Capture and Concentration with Quinones Using Alcohol Additives", *J. Am. Chem. Soc.* **144**, 14161 (2022). <https://doi.org/10.1021/jacs.2c04044>
- ²⁴M.D. Eisaman, L. Alvarado, D. Larner, P. Wang, B. Garg, and K.A. Littau, "CO₂ separation Using Bipolar Membrane Electrodialysis", *Energy Environ. Sci.* **4**, 1319 (2011). <https://doi.org/10.1039/c0ee00303d>
- ²⁵M.D. Eisaman, L. Alvarado, D. Larner, P. Wang, and K.A. Littau, "CO₂ Desorption Using High-Pressure Bipolar Membrane Electrodialysis", *Energy & Environmental Science* **4**, (2011). <https://doi.org/10.1039/c1ee01336j>
- ²⁶M. Rahimi, G. Catalini, M. Puccini, and T.A. Hatton, "Bench-Scale Demonstration of CO₂ Capture with an Electrochemically Driven Proton Concentration Process", *RSC Advances* **10**, 16832 (2020). <https://doi.org/10.1039/d0ra02450c>
- ²⁷X. Li, X. Zhao, Y. Liu, T.A. Hatton, and Y. Liu, "Redox-Tunable Lewis Bases for Electrochemical Carbon Dioxide Capture", *Nature Energy* **7**, 1065 (2022). <https://doi.org/10.1038/s41560-022-01137-z>
- ²⁸S. Jin, M. Wu, Y. Jing, R.G. Gordon, and M.J. Aziz, "Low Energy Carbon Capture Via Electrochemically Induced pH Swing with Electrochemical Rebalancing", *Nat. Commun.* **13**, 2140 (2022). <https://doi.org/10.1038/s41467-022-29791-7>
- ²⁹H. Seo, M. Rahimi, and T.A. Hatton, "Electrochemical Carbon Dioxide Capture and Release with a Redox-Active Amine", *J. Am. Chem. Soc.* **144**, 2164 (2022). <https://doi.org/10.1021/jacs.1c10656>
- ³⁰H. Seo and T.A. Hatton, "Electrochemical Direct Air Capture of CO₂ Using Neutral Red as Reversible Redox-Active Material", *Nat. Commun.* **14**, 313 (2023). <https://doi.org/10.1038/s41467-023-35866-w>
- ³¹S. Pang, S. Jin, F. Yang, M. Alberts, L. Li, D. Xi, R.G. Gordon, P. Wang, M.J. Aziz, and Y. Ji, "A Phenazine-Based High-Capacity and High-Stability Electrochemical CO₂ Capture Cell with Coupled Electricity Storage", *Nature Energy* **8**, 1126 (2023). <https://doi.org/10.1038/s41560-023-01347-z>
- ³²L. Luo, L. Hou, Y. Liu, K. Wu, Y. Zhu, H. Lu, and B. Liang, "Regeneration of Na₂Q in an Electrochemical CO₂ Capture System", *Energy & Fuels* **35**, 12260 (2021). <https://doi.org/10.1021/acs.energyfuels.1c00960>

- ³³S. Jin, Y. Jing, D.G. Kwabi, Y. Ji, L. Tong, D. De Porcellinis, M.A. Goulet, D.A. Pollack, R.G. Gordon, and M.J. Aziz, "A Water-Miscible Quinone Flow Battery with High Volumetric Capacity and Energy Density", *ACS Energy Letters* **4**, 1342 (2019). <https://doi.org/10.1021/acsenergylett.9b00739>
- ³⁴Y. Ji, M.A. Goulet, D.A. Pollack, D.G. Kwabi, S. Jin, D. Porcellinis, E.F. Kerr, R.G. Gordon, and M.J. Aziz, "A Phosphonate-Functionalized Quinone Redox Flow Battery at near-Neutral pH with Record Capacity Retention Rate", *Advanced Energy Materials* **9**, 1900039 (2019). <https://doi.org/10.1002/aenm.201900039>
- ³⁵M. Rahimi, G. Catalini, S. Hariharan, M. Wang, M. Puccini, and T.A. Hatton, "Carbon Dioxide Capture Using an Electrochemically Driven Proton Concentration Process", *Cell Reports Physical Science* **1**, 100033 (2020). <https://doi.org/10.1016/j.xrpp.2020.100033>
- ³⁶L. Yan, J. Bao, Y. Shao, and W. Wang, "An Electrochemical Hydrogen-Looping System for Low-Cost CO₂ Capture from Seawater", *ACS Energy Letters* **7**, 1947 (2022). <https://doi.org/10.1021/acsenergylett.2c00396>
- ³⁷B.T. Huskinson, M.P. Marshak, C. Suh, S. Er, M.R. Gerhardt, C.J. Galvin, X. Chen, A. Aspuru-Guzik, R.G. Gordon, and M.J. Aziz, "A Metal-Free Organic-Inorganic Aqueous Flow Battery", *Nature* **505**, 195 (2014). <https://doi.org/10.1038/nature12909>
- ³⁸K. Lin, Q. Chen, M.R. Gerhardt, L. Tong, S.B. Kim, L. Eisenach, A.W. Valle, D. Hardee, R.G. Gordon, M.J. Aziz, and M.P. Marshak, "Alkaline Quinone Flow Battery", *Science* **349**, 1529 (2015). <https://doi.org/10.1126/science.aab3033>
- ³⁹Y. Jing, E.W. Zhao, M.A. Goulet, M. Bahari, E.M. Fell, S. Jin, A. Davoodi, E. Jonsson, M. Wu, C.P. Grey, R.G. Gordon, and M.J. Aziz, "In Situ Electrochemical Recomposition of Decomposed Redox-Active Species in Aqueous Organic Flow Batteries", *Nat. Chem.* **14**, 1103 (2022). <https://doi.org/10.1038/s41557-022-00967-4>
- ⁴⁰B. Hu, J. Luo, M. Hu, B. Yuan, and T.L. Liu, "A pH-Neutral, Metal-Free Aqueous Organic Redox Flow Battery Employing an Ammonium Anthraquinone Anolyte", *Angew. Chem. Int. Ed.* **58**, 16629 (2019). <https://doi.org/10.1002/anie.201907934>
- ⁴¹E.F. Kerr, Z. Tang, T.Y. George, S. Jin, E.M. Fell, K. Amini, Y. Jing, M. Wu, R.G. Gordon, and M.J. Aziz, "High Energy Density Aqueous Flow Battery Utilizing Extremely Stable, Branching-Induced High-Solubility Anthraquinone near Neutral pH", *ACS Energy Letters* **8**, 8 (2023). <https://doi.org/https://doi.org/10.1021/acsenergylett.2c01691>
- ⁴²Y. Marcus, "Tetraalkylammonium Ions in Aqueous and Non-Aqueous Solutions", *Journal of Solution Chemistry* **37**, 1071 (2008). <https://doi.org/10.1007/s10953-008-9291-1>
- ⁴³J. Wang and T. Hou, "Recent Advances on Aqueous Solubility Prediction", *Combinatorial Chemistry & High Throughput Screening* **14**, 11 (2011). <https://doi.org/10.2174/13862071179550831>
- ⁴⁴Y. Zhu, Y. Li, Y. Qian, L. Zhang, J. Ye, X. Zhang, and Y. Zhao, "Anthraquinone-Based Anode Material for Aqueous Redox Flow Batteries Operating in Nondemanding Atmosphere", *Journal of Power Sources* **501**, 229984 (2021). <https://doi.org/10.1016/j.jpowsour.2021.229984>
- ⁴⁵J. Seravalli and S.W. Ragsdale, "13C NMR Characterization of an Exchange Reaction between CO and CO₂ Catalyzed by Carbon Monoxide Dehydrogenase", *Biochemistry* **47**, 12 (2008). <https://doi.org/https://doi.org/10.1021/bi8004522>
- ⁴⁶B. Hu, C. DeBruler, Z. Rhodes, and T.L. Liu, "Long-Cycling Aqueous Organic Redox Flow Battery (AORFB) toward Sustainable and Safe Energy Storage", *J. Am. Chem. Soc.* **139**, 1207 (2017). <https://doi.org/10.1021/jacs.6b10984>
- ⁴⁷E.S. Beh, D. De Porcellinis, R.L. Gracia, K.T. Xia, R.G. Gordon, and M.J. Aziz, "A Neutral pH Aqueous Organic-Organometallic Redox Flow Battery with Extremely High Capacity Retention", *ACS Energy Letters* **2**, 639 (2017). <https://doi.org/10.1021/acsenergylett.7b00019>
- ⁴⁸A.T. Bui, N.A. Hartley, A.J.W. Thom, and A.C. Forse, "Trade-Off between Redox Potential and the Strength of Electrochemical CO₂ Capture in Quinones", *J. Phys. Chem. C Nanomater. Interfaces* **126**, 14163 (2022). <https://doi.org/10.1021/acs.jpcc.2c03752>
- ⁴⁹A.M. Zito, D. Bím, S. Vargas, A.N. Alexandrova, and J.Y. Yang, "Computational and Experimental Design of Quinones for Electrochemical CO₂ Capture and Concentration", *ACS Sustainable Chemistry & Engineering* **10**, 11387 (2022). <https://doi.org/10.1021/acssuschemeng.2c03463>
- ⁵⁰L. Arnaut, "Pharmacokinetics," in *Chemical Kinetics* (2021), Elsevier, pp. 441. <https://doi.org/10.1016/b978-0-444-64039-0.00013-3>
- ⁵¹D.H. Apaydin, E.D. Glowacki, E. Portenkirchner, and N.S. Sariciftci, "Direct Electrochemical Capture and Release of Carbon Dioxide Using an Industrial Organic Pigment: Quinacridone", *Angew. Chem. Int. Ed. Engl.* **53**, 6819 (2014). <https://doi.org/10.1002/anie.201403618>

⁵²L.T.C. J. R. Miller, G. L. Closs, "Intramolecular Long-Distance Electron Transfer in Radical Anions. The Effects of Free Energy and Solvent on Teh Reaction Rates", *J. Am. Chem. Soc.* **106**, 3 (1984).
<https://doi.org/https://doi.org/10.1021/ja00322a058>

⁵³M. Rahimi, S.M. Moosavi, B. Smit, and T.A. Hatton, "Toward Smart Carbon Capture with Machine Learning", *Cell Reports Physical Science* **2**, 100396 (2021). <https://doi.org/10.1016/j.xcrp.2021.100396>

TOC graphic

